THE JOURNAL OF BIOLOGICAL CHEMISTRY VOL. 288, NO. 20, pp. 14080–14086, May 17, 2013

The Molecular Basis of K^+ Exclusion by the *Escherichia coli* Ammonium Channel AmtB*

Received for publication, January 30, 2013, and in revised form, March 27, 2013 Published, JBC Papers in Press, April 1, 2013, DOI 10.1074/jbc.M113.457952

Jason A. Hall[‡1] **and Dalai Yan**[§]

From the [‡]*Division of Biological Sciences, University of California San Diego, La Jolla, California 92093-0374 and the* [§]*Department of Microbiology and Immunology, Indiana University School of Medicine, Indianapolis, Indiana 46202-5120*

Background: The Amt family of ammonium channels does not conduct K^+.
Results: *E. coli* AmtB variants carrying certain mutations in the conserved twin-histidine element transport K^+ against a concentration gradient.
Conclusion: The twin-histidine element functions as a filter that prevents K^+ conduction.
Significance: These findings provide insight into the transport mechanism of Amt channels and the ammonium species (NH_3 or NH_4^+) that serves as their substrate.

Members of the Amt family of channels mediate the transport of ammonium. The form of ammonium, NH_3 or NH_4^+, carried by these proteins remains controversial, and the mechanism by which they select against K^+ ions is unclear. We describe here a set of *Escherichia coli* AmtB proteins carrying mutations at the conserved twin-histidine site within the conduction pore that have altered substrate specificity and now transport K^+. Subsequent work established that AmtB-mediated K^+ uptake occurred against a concentration gradient and was membrane potential-dependent. These findings indicate that the twin-histidine element serves as a filter to prevent K^+ conduction and strongly support the notion that Amt proteins transport cations (NH_4^+ or, in mutant proteins, K^+) rather than NH_3 gas molecules through their conduction pores.

Ammonium (used to designate NH_3 and NH_4^+) is the preferred nitrogen source of many organisms, making the manner by which it traverses biological membranes of great physiological importance. The uncharged form, NH_3, diffuses across lipid bilayers more than 35 times faster than water (1). When the rate of NH_3 diffusion becomes growth limiting protein-mediated transport of ammonium by the Amt family of channels is required (2–5). Still subject to debate is the transport mechanism of these proteins and the species of ammonium that serves as their substrate. Based on structural studies and numerous molecular dynamic simulations (6–11), it has been argued that Amt family members are passive channels that facilitate downhill movement of NH_3. We hold the opposite view, supported by the research efforts of other groups (3, 12–20), that these proteins function as active channels that mediate electrogenic ammonium uptake against a concentration gradient. Mechanisms of electrogenic transport that have been suggested include conduction of the membrane-impermeant protonated form of ammonium, NH_4^+, and the cotransport of NH_3 and H^+ (2, 3, 5, 12, 13, 16–21).

Members of the Amt family function as homotrimers (22). Structural studies indicate that these proteins and their only known homologs, the Rhesus (Rh) proteins, have a conduction pore on each monomeric subunit (7, 11, 21, 23–25) (Fig. 1). Positioned near the center of each of these otherwise hydrophobic pores is a pair of conserved histidines. It has been proposed that this twin-histidine element plays a critical role in mediating substrate transport (7, 11, 28). However, recent work by one of us demonstrated that the *E. coli* AmtB protein can accommodate acidic residues at one or both positions of its His^{168}/His^{318} twin-histidine pairing while retaining good to excellent ammonium transport activity (14). This finding led us to question why the twin-histidine element is conserved within the Amt family. Here, we report that certain AmtB twin-histidine variants are gain-of-function mutants that conduct K^+, a cation having an ionic radius similar to that of NH_4^+ but normally not transported by Amt proteins (17, 18, 29, 30). Our analysis shows that the twin-histidine element serves as a substrate selectivity filter and leads us to suggest that Amt channels utilize an electrogenic transport mechanism in which ammonium crosses the phenyl ring constriction as NH_4^+, deprotonates and traverses the conduction pore in close association with its H^+, and finally reprotonates prior to entering the cytoplasm.

EXPERIMENTAL PROCEDURES

Bacterial Strains and Growth Media—Unless noted otherwise, all strains used in this work are derivatives of the prototrophic *E. coli* K-12 strain NCM3722 (3, 31). Strains NCM4236 (*tesB*::kan), NCM4590 (*amtB*::kan), NCM4833 (*amtB*^{H318D} *tesB*::kan), NCM4889 (*amtB*^{H168D} *tesB*::kan), and NCM4892 (*amtB*^{H168D,H318E} *tesB*::kan) have been described (3, 14, 32). Strain NCM5020 (Δ*kdpA* Δ*trkA kup*::cat) was constructed using successive rounds of P1 phage transduction and FLP recombinase-mediated resistance gene excision of *kdpA*::kan and then *trkA*::kan insertions (derived from Keio collection strains JW0686-5 and JW3251-2, respectively) (33), followed by a third transduction with P1 phage grown on strain

* This work was supported by National Institutes of Health Grant GM38361 (to Sydney Kustu).
[1] To whom correspondence should be addressed: Section of Molecular Biology, Division of Biological Sciences, University of California San Diego, 9500 Gilman Dr., La Jolla, CA 92093-0374. Tel.: 510-642-2546; E-mail: jahall@ucsd.edu.

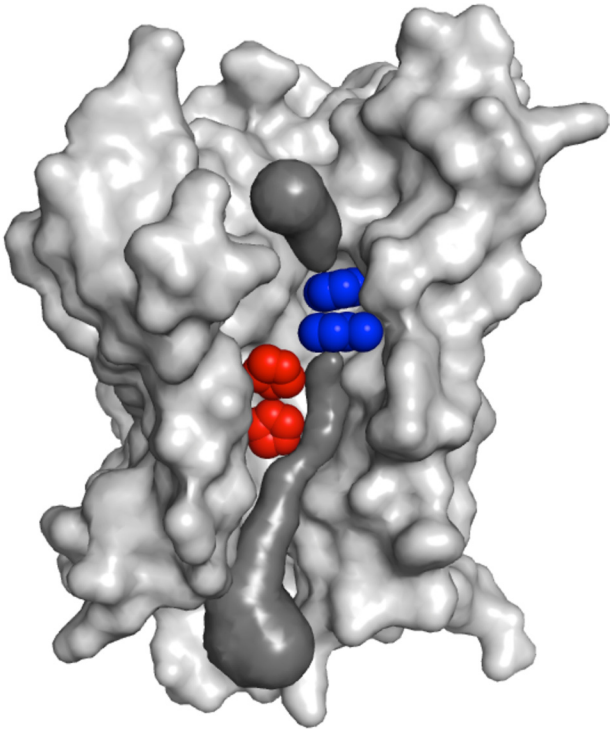

FIGURE 1. **Substrate conduction path of *E. coli* AmtB.** The AmtB monomer as viewed from the membrane, with the periplasmic surface at the *top* and cytoplasmic surface at the *bottom*. Forward facing transmembrane helices have been removed to reveal the substrate transport path (modeled in *dark gray*). Components of the conserved twin-histidine element (His^{168} on the *top* and His^{318} on the *bottom*) are highlighted in *red*. A constriction composed of two conserved and presumably mobile phenylalanine residues (Phe^{107} on the *top* and Phe^{215} on the *bottom*) that separates the periplasmic vestibule of the transport pathway from the conduction pore is shown in *blue*. Whether ammonium crosses the phenyl ring constriction and traverses the conduction pore as NH_3 or NH_4^+ remains a point of debate. The AmtB model was created from Protein Data Bank entry 2NS1 (26) using PyMOL, and the substrate conduction pathway was visualized using the program CAVER (27).

NCM5019 (MG1655 *kup*::cat). Selected *amtB* alleles were introduced into strain NCM5020 by P1 phage transduction using *amtB*::kan or by linkage to *tesB*::kan. Strains NCM5030 (NCM5020 Δ*glnK* $amtB^{H318D}$ *tesB*::kan) and NCM5031 (NCM5020 Δ*glnK* $amtB^{H168D,H318E}$ *tesB*::kan) were constructed by first introducing mutant *amtB tesB*::kan fragments into strain NCM4589 (NCM3722 Δ*glnK*) using previously described methods (3, 14, 32), and then moving the Δ*glnK* $amtB^{H318D}$ and Δ*glnK* $amtB^{H168D,H318E}$ lesions into the NCM5020 strain background by P1 phage transduction using the close linkage of *glnK* and *amtB* to *tesB*::kan. Genetic manipulations were confirmed by PCR and sequencing. All *amtB* alleles were studied in single copy on the *E. coli* chromosome.

Strains in the NCM3722 background were maintained on LB plates, and strains in the NCM5020 background were maintained on LB plates containing 50 mM KCl. K^+-based formulations of N^-C^- minimal medium, Neidhardt's MOPS medium, and Neidhardt's MES medium contain ~200, 28, and 20 mM K^+, respectively (3, 34, 35). Na^+-based formulations of these defined media were prepared by replacing all K^+-containing components with their Na^+-containing counterparts.

Growth Assays—For strain growth illustrated in Fig. 2, cells grown in LB medium were diluted 100-fold into either K^+-based or Na^+-based N^-C^- minimal medium containing 0.4% glucose and 5 mM NH_4Cl. After overnight incubation, cells were diluted to an $A_{600} = 0.01$ (>100-fold dilution) into either K^+-based or Na^+-based N^-C^- medium containing 0.04% glucose and 3 mM glutamine. Glutamine supports good growth as a sole source of nitrogen when cells are cultivated in this medium but its use as a sole nitrogen source elicits the nitrogen limitation response, resulting in the expression of all genes, including *amtB*, under control of nitrogen regulatory protein C (NtrC) (36–38). Growth was monitored by changes in absorbance at 600 nm. Strain growth was carried out with aeration at 37 °C. All Na^+-based N^-C^- medium was supplemented with 1 mM KCl to avoid K^+-limiting growth conditions.

For strain growth illustrated in Fig. 4, cells grown in LB medium containing 100 mM KCl were diluted 100-fold into Na^+-based N^-C^- medium supplemented with 0.4% glucose, 5 mM NH_4Cl, and 100 mM KCl. After these cultures reached saturation they were again diluted 100-fold into the same Na^+-based N^-C^- medium, except with 3 mM glutamine replacing NH_4Cl as the nitrogen source. Following overnight incubation, cultures were finally diluted 200-fold into Na^+-based N^-C^- medium supplemented with 0.4% glucose, 3 mM glutamine, and a mixture of KCl and NaCl (combined concentration of 100 mM). Growth was monitored by changes in absorbance at 600 nm. Strain growth was carried out with aeration at 37 °C.

Growth at low NH_3 concentrations (Fig. 3) was performed as previously described (14) with the following differences: cells were first adapted to minimal medium on Na^+-based Neidhardt's MOPS medium (pH 7.4) and subsequently acclimated to growth at low pH by inoculation into Na^+-based Neidhardt's MES medium (pH 5.5); all adaptive media contained 1 mM KCl; and cells were finally diluted into either K^+-based Neidhardt's MES medium (pH 5.5) supplemented with 1 mM KCl, or Na^+-based Neidhardt's medium (pH 5.5) supplemented with 0.1 mM KCl and 0.9 mM NaCl.

Expression and accumulation levels of mutant proteins relative to wild-type AmtB have been reported (14). The three AmtB variants studied here were produced in amounts similar to that of the wild-type strain (60–100%) when glutamine served as the sole nitrogen source (Fig. 2 and Figs. 4–7). However, whereas $AmtB^{H168D}$ and $AmtB^{H318D}$ accumulated to 30–40% wild-type levels under this growth condition, $AmtB^{H168D,H318E}$ was present in amounts ≤5% of its wild-type counterpart. Similar expression and accumulation patterns were found for these three AmtB variants when low NH_3 medium was used for growth studies (Fig. 3).

Transport Assays—Strains were grown in LB medium containing 100 mM KCl and, after overnight incubation, diluted 100-fold into Na^+-based N^-C^- medium supplemented with 0.4% glucose, 5 mM NH_4Cl, and 100 mM KCl. After these cultures reached saturation they were again diluted 100-fold into the same Na^+-based N^-C^- medium, except with 3 mM glutamine replacing NH_4Cl as the nitrogen source. Cells cultivated under these conditions were grown to exponential phase ($A_{600} = 0.3–0.6$), harvested by centrifugation, and resuspended in Na^+-based N^-C^- medium containing 100 mM NaCl. For determination of cytoplasmic K^+ pools, cells were collected and processed for inductively coupled plasma atomic emission

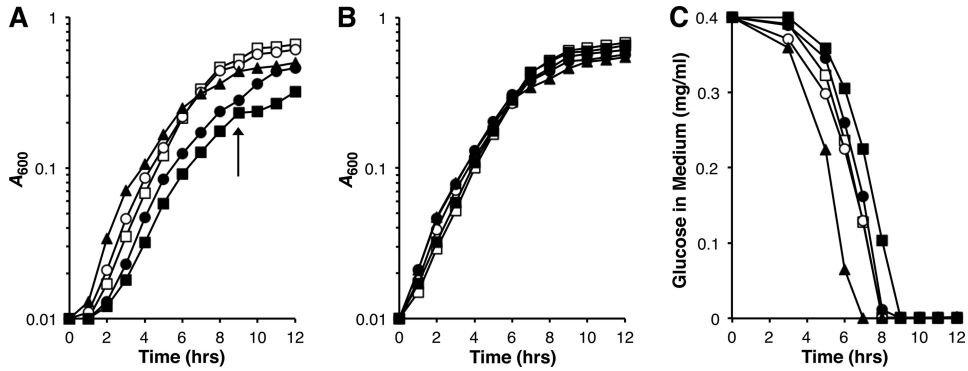

FIGURE 2. **Effect of K^+ on AmtB twin-histidine variant strain growth.** *A* and *B*, strains were cultivated in either K^+-based N^-C^- minimal medium (contains 200 mM K^+) (*A*) or Na^+-based N^-C^- minimal medium supplemented with 1 mM KCl (*B*). All media contained 0.04% glucose and 3 mM glutamine. AmtB is expressed under these growth conditions (see "Experimental Procedures" for details). Strain genotypes were wild-type (○), *amtB*-null (□), H168D (▲), H318D (●), and H168D,H318E (■). The arrow in *A* denotes the point at which the glucose supply is exhausted by cells expressing $AmtB^{H168D,H318E}$ (see *C*), and the tricarboxylic acid cycle intermediates derived from glutamine begin to be used as the source of carbon. The data, from a single experiment, are representative of findings made in three independent trials. *C*, glucose consumption by strains illustrated in *A*. Culture medium glucose concentrations were determined at various times during growth. The times at which strains exhaust their glucose supply are closely approximated by their diauxic shift points in *A*: 7 h for H168D, 8 h for *amtB*-null, 8 h for wild type, 8 h for H318D, 9 h for H168D,H318E. Cell yield per glucose consumed values (shown below in units of A_{600}/mg of glucose per ml) at the diauxic shift point for each strain were 1.2 ± 0.12 for *amtB*-null, 1.1 ± 0.063 for wild-type, 0.73 ± 0.052 for H168D, 0.62 ± 0.029 for H318D, and 0.55 ± 0.025 for H168D,H318E. Cell yield per glucose consumed values are reported as means ± S.D. for three independent experiments. Symbols used for strain genotypes in *C* are identical to those in *A* and *B*.

spectroscopy (ICP-AES)[2] (see below). To analyze K^+ uptake, resuspended cells were washed twice and finally suspended at an A_{600} = 1.0 in Na^+-based N^-C^- medium containing 100 mM NaCl, and then treated with 5 mM 2,4-dinitrophenol for 30 min. Treatment with this protonophore results in the rapid loss of cellular K^+ (39, 40). K^+-depleted cells were harvested, washed twice with Na^+-based N^-C^- medium supplemented with 100 mM NaCl, resuspended at an A_{600} = 1.0 in the same medium supplemented with 0.2% glucose, and held on ice until use. To initiate tests of K^+ transport, cell suspensions were preincubated for 20 min at 37 °C prior to the addition of an equal volume of Na^+-based N^-C^- medium supplemented with 0.2% glucose and suitable mixtures of KCl, NH_4Cl, and NaCl (combined concentration of 100 mM). After a 1 min incubation aliquots were collected on Millipore filters (0.45-μm pore size; type HAWP), rinsed twice with 5 ml of Na^+-based N^-C^- medium supplemented with 100 mM NaCl, and dried. Washed cells (on the filter) were then incubated at room temperature (~25 °C) for 1 h in 5 ml of 1 M HNO_3 containing 50 μM NaCl to extract K^+. Samples were cleared of cell debris by passage through Millipore filters (0.45-μm pore size; type HAWP) and analyzed for K^+ by ICP-AES. To determine whether AmtB-mediated K^+ transport required an energy source (Fig. 7*A*), glucose was eliminated from all assay buffer preparations. For assays with carbonyl cyanide *m*-chlorophenylhydrazone (CCCP), this compound or an equal volume of ethanol vehicle was added 5 min prior to the initiation of K^+ uptake tests. Strain growth, K^+ depletion, and K^+ uptake assays were carried out with aeration at 37 °C.

Apparent kinetic constants (half-saturation constant values and maximal transport rates) for AmtB-mediated K^+ uptake were estimated by curve fitting initial transport rates to the Michaelis-Menten equation using the program CurveExpert Professional, version 1.6.2. The concentration range of K^+ used to approximate these kinetic constants was 0.5–50 mM. Inhibition constant (K_i) values for ammonium inhibition of AmtB-mediated K^+ transport were determined using linear Dixon plots (41), with the assumption of competitive inhibition between ammonium and K^+. For energy requirement assays and K_i determinations (Fig. 7), K^+ was present at twice half-saturation constant values for $AmtB^{H318D}$ and $AmtB^{H168D,H318E}$ in the *glnK*$^+$ background, and 40 mM for $AmtB^{H318D}$ and $AmtB^{H168D,H318E}$ in the *glnK* background. Transport values measured in the absence of ammonium using these K^+ concentrations were 180 ± 38 nmol/ml per A_{600} per min for $AmtB^{H318D}$ in the *glnK*$^+$ background, 210 ± 51 nmol/ml per A_{600} per min for $AmtB^{H168D,H318E}$ in the *glnK*$^+$ background, 140 ± 21 nmol/ml per A_{600} per min for $AmtB^{H318D}$ in the *glnK* background, and 96 ± 6.3 nmol/ml per A_{600} per min for $AmtB^{H168D,H318E}$ in the *glnK* background. The concentration range of ammonium used to approximate K_i values was 1 μM to 10 mM.

Glucose Determination—Samples from cultures illustrated in Fig. 2*A* were subjected to filtration (0.22-μm pore size; Millipore type Millex-GV) to remove cells. Glucose concentrations in cell-free medium were determined enzymatically using a glucose oxidase/peroxidase-coupled assay monitoring the oxidation of *o*-dianisidine (Sigma-Aldrich product GAGO-20).

RESULTS

K^+-dependent Growth Defect in AmtB Twin-histidine Variant Strains—A number of *E. coli* AmtB mutant proteins carrying acidic residues at the His^{168}/His^{318} twin-histidine site cause a pronounced growth defect when expressed under nitrogen-limiting conditions in media devoid of ammonium and of high K^+ content (Fig. 2, *A* and *C*). This defect is characterized by a decreased carbon yield relative to both the wild-type and *amtB*-null strains. We reasoned that the twin-histidine variants exhibiting the growth defect were wasting energy in the futile active transport of K^+. Several mutants were selected to test this hypothesis. Two of these, $AmtB^{H168D}$ and $AmtB^{H318D}$, have near wild-type ammonium transport activity even in the

[2] The abbreviations used are: ICP-AES, inductively coupled plasma atomic emission spectroscopy; CCCP, carbonyl cyanide *m*-chlorophenylhydrazone.

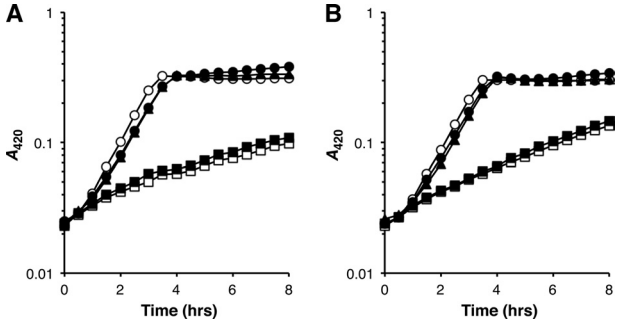

FIGURE 3. **Growth of AmtB twin-histidine variant strains at low NH_3.** Strain growth in low NH_3 medium (0.5 mM NH_4Cl, 0.1% glucose (pH 5.5)) containing 21 mM K^+ (*A*) or 0.1 mM K^+ (*B*) is shown. The absence of AmtB-mediated conductance of ammonium under these culture conditions results in a pronounced growth defect (3, 37). Strain genotypes were wild-type (○), *amtB*-null (□), H168D (▲), H318D (●), and H168D,H318E (■). Strain doubling times (in minutes) derived from these growth curves are as follows: 48 and 47 for wild-type at K^+ concentrations of 21 mM and 0.1 mM, respectively; 320 and 210 for *amtB*-null at K^+ concentrations of 21 mM and 0.1 mM, respectively; 55 and 53 for H168D at K^+ concentrations of 21 mM and 0.1 mM, respectively; 55 and 55 for H318D at K^+ concentrations of 21 mM and 0.1 mM, respectively; 280 and 200 for H168D,H318E at K^+ concentrations of 21 mM and 0.1 mM, respectively. The data, each from single experiments, are representative of findings made in at least three independent trials.

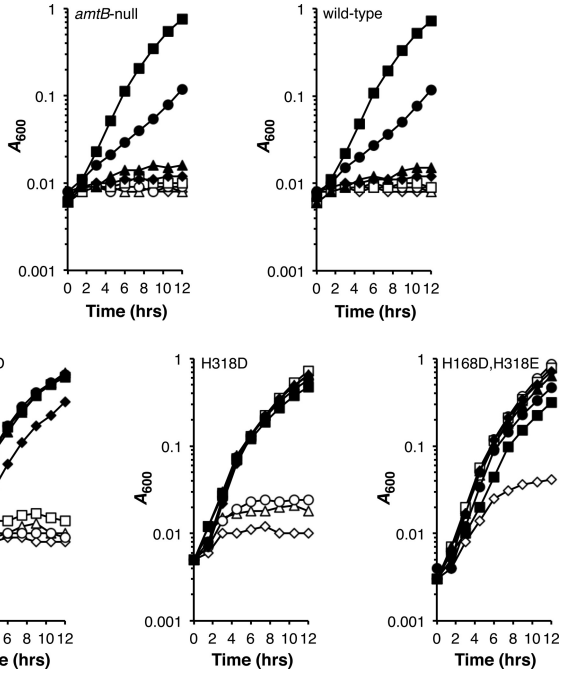

FIGURE 4. **Dependence of strain growth on K^+ concentration.** Strains were grown under AmtB-expressing conditions (Na^+-based N^-C^- minimal medium containing 0.4% glucose, and 3 mM glutamine) in medium supplemented with varying concentrations of KCl (0.5 mM (◇), 1 mM (△), 2 mM (○), 5 mM (□), 10 mM (◆), 20 mM (▲), 50 mM (●), and 100 mM (■)). Growth medium isotonicity was maintained by the addition of NaCl such that the total KCl/NaCl supplement equaled 100 mM. All *amtB* alleles were carried in the *kdp trk kup* strain background. The data, from a single experiment, are representative of findings made in three independent trials.

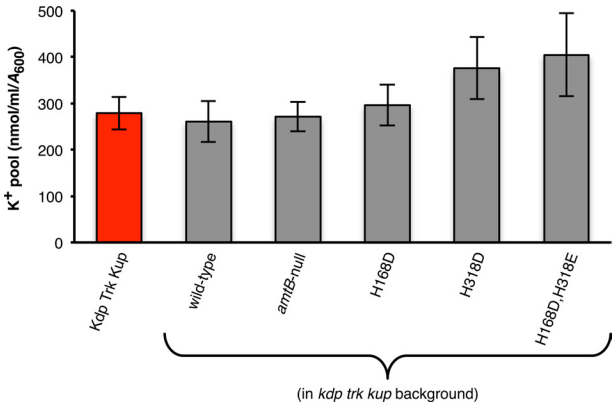

FIGURE 5. **Cytoplasmic K^+ pools.** Intracellular K^+ levels in strains grown under AmtB-expressing conditions (Na^+-based N^-C^- minimal medium supplemented with 0.4% glucose, 3 mM glutamine, and 100 mM KCl). All *amtB* alleles were carried in the *kdp trk kup* strain background. For comparison purposes, the cytoplasmic K^+ pool of the prototrophic *E. coli* K-12 parental strain NCM3722 (Kdp Trk Kup) (31) is shown (*red bar*). Values reported are means ± S.D. (*error bars*) for at least three independent experiments.

presence of ~20 mM K^+ (Fig. 3 and Ref. 14). Like wild-type AmtB, the $AmtB^{H168D}$ protein also transports the ammonium analog methylammonium (used to designate CH_3NH_2 and $CH_3NH_3^+$) in the absence of K^+, whereas $AmtB^{H318D}$ does not (14). A third mutant, $AmtB^{H168D,H318E}$, that exhibits neither ammonium nor methylammonium transport activity even at low K^+ (Fig. 3 and Ref. 14) was also examined. Studies conducted on cells expressing these variants showed that the growth defect was eliminated if Na^+ replaced most of the K^+ in the culture medium (1 mM K^+ supplied to avoid K^+-limiting growth conditions) (Fig. 2*B*).

AmtB Twin-histidine Variants Conduct K^+—Having established a link between the external K^+ concentration and the growth defect observed in certain twin-histidine mutants, we next looked to see whether this defect resulted from AmtB-mediated inward K^+ leakage. A strain lacking the three major K^+ import systems (Kdp, Trk, and Kup) was constructed for this work. In the absence of these transport systems *E. coli* possesses only a residual K^+ uptake activity and requires an elevated concentration of this cation for growth (39, 40). We found that the *kdp trk kup* triple mutant failed to grow appreciably on media containing less than ~50 mM K^+, and expression of wild-type AmtB had no effect on this growth phenotype (Fig. 4; compare *amtB*-null and wild-type strains). Expression of $AmtB^{H168D}$, $AmtB^{H318D}$, or $AmtB^{H168D,H318E}$, on the other hand, reduced the K^+ requirement to ~10, 5, and 1 mM, respectively.

The ability of AmtB to conduct K^+ was also assayed directly using ICP-AES. Initial experiments indicated that cytoplasmic K^+ pools of *kdp trk kup* triple mutants expressing a twin-histidine variant protein, in particular $AmtB^{H318D}$ or $AmtB^{H168D,H318E}$, were not only higher than their wild-type AmtB-expressing and *amtB*-null counterparts, but also larger than that of a wild-type AmtB-expressing strain carrying the Kdp, Trk, and Kup systems (Fig. 5). We next depleted each of these strains of their K^+ to study the net uptake of this cation. As expected, the K^+ transport rate of a *kdp trk kup* triple mutant expressing wild-type AmtB was no better than that of an otherwise isogenic *amtB*-null strain (Fig. 6*A*). Only a slight improvement (<2-fold) in K^+ uptake was observed when $AmtB^{H168D}$ was expressed in this background. The initial K^+ transport rates of wild-type AmtB and $AmtB^{H168D}$ were linearly proportional to the external K^+ concentration over the range tested (up to 50 mM) and markedly lower than the combined activities of Trk and Kup (Kdp not expressed under the conditions (100 mM K^+ in the growth medium) used for this assay; Refs. 39, 40).

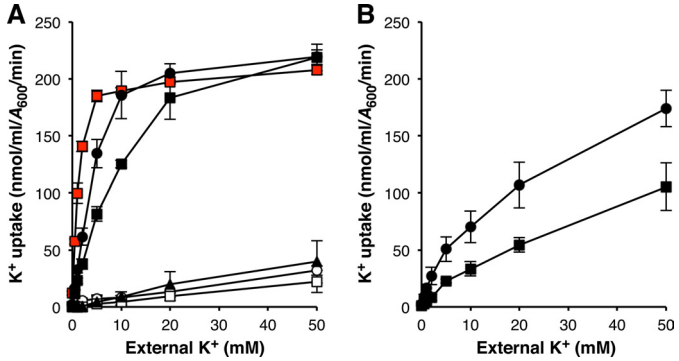

FIGURE 6. **Kinetics of AmtB-mediated K^+ transport.** *A*, initial (1 min) rates of AmtB-mediated K^+ uptake were measured in K^+-depleted *kdp trk kup* cells. Strain genotypes were wild-type (○), *amtB*-null (□), H168D (▲), H318D (●), and H168D,H318E (■). The K^+ uptake activity of the prototrophic *E. coli* K-12 parental strain NCM3722 (31) is shown (*solid red squares*). *B*, initial (1 min) rates of K^+ uptake were measured in K^+-depleted *kdp trk kup glnK* cells expressing $AmtB^{H318D}$ (●) and $AmtB^{H168D,H318E}$ (■). Values reported in *A* and *B* are means ± S.D. (*error bars*) for at least three independent experiments. Kinetic constants for K^+ transport determined from the data shown in *A* are reported under "Results" as means ± S.D. Half-saturation constant values and maximal transport rates determined from the data shown in *B* were 26 ± 9.1 mM and 260 ± 8.5 nmol/ml per A_{600} per min for $AmtB^{H318D}$ and 60 ± 21 mM and 230 ± 85 nmol/ml per A_{600} per min for $AmtB^{H168D,H318E}$.

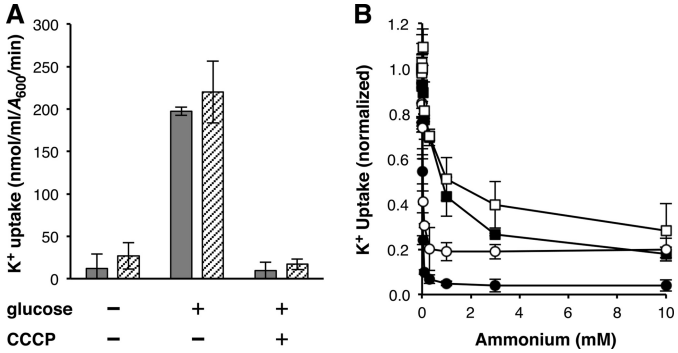

FIGURE 7. **Inhibition of AmtB-mediated K^+ transport.** *A*, initial (1 min) rates of K^+ uptake by $AmtB^{H318D}$ (*shaded bars*) and $AmtB^{H168D,H318E}$ (*hatched bars*) measured in K^+-depleted *kdp trk kup* cells in the presence and absence of an energy source (0.2% glucose) and protonophore (10 μM CCCP). Values shown are means ± S.D. (*error bars*) of three independent experiments. *B*, initial (1 min) uptake rates of K^+ by $AmtB^{H318D}$ (● and ○) and $AmtB^{H168D,H318E}$ (■ and □) determined in K^+-depleted *kdp trk kup* cells (*shaded symbols*) or K^+-depleted *kdp trk kup glnK* cells (*open symbols*) in the presence of varying concentrations of ammonium. Data from three separate trials were normalized to transport values measured in the absence of ammonium and are shown as means ± S.D. (*error bars*). Inhibition constants (K_i) for ammonium determined from each of these independent experiments are reported under "Results" as means ± S.D. Assay K^+ concentrations for *A* and *B* and transport values measured in the absence of ammonium for *B* are reported under "Experimental Procedures".

$AmtB^{H318D}$ and $AmtB^{H168D,H318E}$, on the other hand, exhibited considerable K^+ uptake activity. These two twin-histidine variants were found to have 5–10-fold higher half-saturation constant values (4.9 ± 0.93 mM and 11 ± 1.4 mM for $AmtB^{H318D}$ and $AmtB^{H168D,H318E}$, respectively) and elevated maximal transport rates (250 ± 6.0 nmol/ml per A_{600} per min and 270 ± 22 nmol/ml per A_{600} per min for $AmtB^{H318D}$ and $AmtB^{H168D,H318E}$, respectively) relative to the aggregate kinetic properties of the Trk and Kup systems (half-saturation constant of 1.1 ± 0.07 mM; maximal transport rate of 210 ± 2.1 nmol/ml per A_{600} per min; also see Ref. 40). Given that a 1 ml *E. coli* culture of $A_{600} = 1$ has a total cell volume of ~3.6 μl (42), we calculate that $AmtB^{H318D}$ and $AmtB^{H168D,H318E}$ concentrate K^+ 3–10-fold during the first min of the transport reaction when K^+ is present at 0.5–10 mM in the external medium.

Inhibition of AmtB-mediated K^+ Transport—We used $AmtB^{H318D}$ and $AmtB^{H168D,H318E}$ as vehicles to analyze the energy requirements of AmtB-mediated K^+ conduction and the effect ammonium has on this transport reaction. The rate of K^+ uptake by these two proteins was reduced 90–95% when the protonophore CCCP was present at a concentration of 10 μM (Fig. 7*A*), indicating that K^+ uptake by AmtB was dependent on the proton motive force, presumably the membrane potential component, across the cytoplasmic membrane. In support of this conclusion is the finding that neither twin-histidine variant conducted K^+ after treatment with 2,4-dinitrophenol, a process that both depletes the cytoplasmic K^+ pool and discharges the proton motive force (39, 40), without subsequent addition of an energy source. Competition tests showed that K^+ transport by these mutant proteins was also reduced in the presence of ammonium (Fig. 7*B*). The inhibitory effect was far greater for $AmtB^{H318D}$ (K_i = 4.9 ± 1.9 μM), which conducts ammonium, than for $AmtB^{H168D,H318E}$ (K_i = 0.77 ± 0.37 mM), which lacks ammonium uptake activity. Because the GlnK protein quickly inactivates AmtB in the presence of micromolar quantities of external ammonium (43), the impact this compound had on AmtB-mediated K^+ transport was also examined in a *kdp trk kup glnK* strain background. Half-saturation constant values for $AmtB^{H318D}$ and $AmtB^{H168D,H318E}$ K^+ uptake were increased ~5-fold when GlnK was not present (Fig. 6*B*). Similar-sized decreases in ammonium inhibition of K^+ transport by $AmtB^{H318D}$ (K_i = 22 ± 5.3 μM) and $AmtB^{H168D,H318E}$ (K_i = 2.9 ± 1.6 mM) were observed in the absence of the GlnK protein (Fig. 7*B*). These results suggest that the uptake of K^+ is influenced by AmtB-GlnK interaction and, when taken together with the observation that $AmtB^{H318D}$ K^+ conduction was strongly inhibited by ammonium, provides support for the idea that K^+ and ammonium share the same transport pathway through AmtB.

DISCUSSION

Controversy remains over the form of ammonium carried by members of the Amt family. Due to the strongly hydrophobic nature of the conduction pore it was proposed that these proteins facilitated diffusion of NH_3 (7, 11). A study of AmtB function in a reconstituted system provided evidence for such a transport mechanism (7), but the findings of that work have been criticized for being interpreted incorrectly and could not be corroborated (4, 44). Other observations question the plausibility of the facilitated NH_3 diffusion model. Quantitative analyses of ammonium flux have shown that this transport mechanism would not sustain the rates of growth observed under the low external ammonium conditions at which Amt proteins operate (15, 44). Also, given that these proteins are active when the internal to external ammonium concentration ratio is >1 (15), facilitated diffusion would lead to the export rather than import of ammonium without the involvement of a linked energy source. The alternative view of ammonium transport holds that Amt channels actively conduct NH_4^+ or cotransport NH_3 and H^+. In support of these mechanisms, all plant

members of the Amt family functionally characterized to date, save for those from the distantly related AMT2 subfamily, have been found to mediate electrogenic ammonium uptake (4, 17, 18, 30, 45, 46). Moreover, Amt proteins from a number of other organisms, including *E. coli*, concentrate methylammonium in a membrane potential-dependent manner (3, 13, 16, 20). That certain AmtB twin-histidine variants conduct K^+ against its concentration gradient (Fig. 6) is compatible with these active transport mechanisms. In addition, because K^+ cannot separate from its charge, our results imply that ammonium migrates through the AmtB pore as either NH_4^+ or as a closely associated NH_3/H^+ pairing (see below). This is in contrast to a net NH_4^+ uptake mechanism that proceeds via a symport reaction in which NH_3 passes through the pore alone while a H^+ follows a separate unidentified transport pathway.

In work presented here, we have described a set of AmtB twin-histidine variants that have altered substrate specificity and now conduct K^+. The spectrum of compounds (methylammonium, ammonium, and K^+) carried by each mutant depends on the position and number of acidic residues present in the conduction pore. Thus, $AmtB^{H168D}$ transports all three compounds, $AmtB^{H318D}$ conducts both ammonium and K^+ but no longer exhibits methylammonium uptake activity, and $AmtB^{H168D,H318E}$ carries only K^+ (Figs. 3, 4 , and 6; and Ref. 14). These findings lead us to conclude that the His^{168}/His^{318} twin-histidine element serves as a substrate selectivity filter that prevents K^+ transport. How might this element enable members of the Amt family to discriminate between K^+ and ammonium? If, as our results predict, ammonium crosses the phenyl ring constriction and enters the conduction pore as NH_4^+ its charge will need to be masked to migrate across this hydrophobic environment. By accepting a H^+ from NH_4^+ and only transferring it back just prior to substrate release into the cytoplasm, a transport mechanism shown to be plausible in a recent simulation study (47), the twin-histidine element allows the H^+ to remain delocalized as it moves in parallel with NH_3 through the conduction pore. The transport of K^+ is prohibited because, unlike NH_4^+ and $CH_3NH_3^+$, this cation is incapable of separating from its charge. Certain acidic amino acid substitutions of the twin-histidine element reduce the need for such charge separation by increasing pore hydrophilicity and, as a consequence, allow K^+ to be carried. It is not clear why these mutations would also cause progressive decreases in $CH_3NH_3^+$ and then NH_4^+ transport. However, the underlying trend suggests that this behavior results from the differences in the manner by which the introduced acidic residues handle H^+ and K^+ as well as changes to the hydrophobic character of the pore.

The strong preference of Amt family members for ammonium over K^+ (3, 17, 18, 29, 30, 48) implies that this selectivity is physiologically important. Our current analysis highlights why these proteins do not carry K^+. The inward leakage of this cation through AmtB, although able to substitute for the K^+ uptake activities of the Trk and Kup systems, is associated with a large energy cost (Fig. 2, *A* and *C*). We suggest that this cost is incurred by the action of two processes. First, K^+ movement across the cytoplasmic membrane is known to play an important role in regulating pH homeostasis (39, 49, 50). Given the elevated K^+ pools found in cells expressing AmtB twin-histidine variants, substantial energy reserves would likely be used to preserve normal intracellular pH. Similarly, energy would be required to maintain the membrane potential that would otherwise be dissipated by illicit AmtB-mediated K^+ conduction. These energy expenditures can prove problematic because members of the Amt family oftentimes need to operate in nutrient-poor environments having high K^+ levels. For instance, the two Amt proteins of *Nitrosopumilus maritimus*, a member of a group of ammonium-oxidizing marine archaea that are key intermediates in the global nitrogen cycle, are likely active in the open ocean where ammonium and K^+ concentrations are $<1\ \mu$M and ~ 10 mM, respectively (51–53). Growth and survival under such energy- and nitrogen-limited conditions would be severely compromised if Amt proteins did not discriminate against K^+.

Acknowledgments—We are grateful to Sydney Kustu for her involvement in all stages of this research project. We thank Terence Hwa for suggesting that AmtB-mediated K^+ leakage was responsible for the growth defect illustrated in Fig. 2A; Paul Brooks at the University of California, Berkeley ICP Spectroscopy Facility for ICP-AES assistance; and Wolfgang Epstein, Hiroshi Nikaido, and Helen Zgurskaya for thoughtful criticisms of the manuscript.

REFERENCES

1. Walter, A., and Gutknecht, J. (1986) Permeability of small nonelectrolytes through lipid bilayer membranes. *J. Membr. Biol.* **90,** 207–217
2. Andrade, S. L., and Einsle, O. (2007) The Amt/Mep/Rh family of ammonium transport proteins. *Mol. Membr. Biol.* **24,** 357–365
3. Fong, R. N., Kim, K. S., Yoshihara, C., Inwood, W. B., and Kustu, S. (2007) The W148L substitution in the *Escherichia coli* ammonium channel AmtB increases flux and indicates that the substrate is an ion. *Proc. Natl. Acad. Sci. U.S.A.* **104,** 18706–18711
4. Javelle, A., Lupo, D., Li, X. D., Merrick, M., Chami, M., Ripoche, P., and Winkler, F. K. (2007) Structural and mechanistic aspects of Amt/Rh proteins. *J. Struct. Biol.* **159,** 243–252
5. Ludewig, U. (2006) Ion transport versus gas conduction: function of AMT/Rh-type proteins. *Transfus. Clin. Biol.* **13,** 111–116
6. Bostick, D. L., and Brooks, C. L. (2007) Deprotonation by dehydration: the origin of ammonium sensing in the AmtB channel. *PLoS Comput. Biol.* **3,** e22
7. Khademi, S., O'Connell, J., 3rd, Remis, J., Robles-Colmenares, Y., Miercke, L. J., and Stroud, R. M. (2004) Mechanism of ammonia transport by Amt/MEP/Rh: structure of AmtB at 1.35 Å. *Science* **305,** 1587–1594
8. Lin, Y., Cao, Z., and Mo, Y. (2009) Functional role of Asp160 and the deprotonation mechanism of ammonium in the *Escherichia coli* ammonia channel protein AmtB. *J. Phys. Chem. B* **113,** 4922–4929
9. Nygaard, T. P., Rovira, C., Peters, G. H., and Jensen, M. Ø. (2006) Ammonium recruitment and ammonia transport by *E. coli* ammonia channel AmtB. *Biophys. J.* **91,** 4401–4412
10. Yang, H., Xu, Y., Zhu, W., Chen, K., and Jiang, H. (2007) Detailed mechanism for AmtB conducting NH_4^+/NH_3: molecular dynamic simulations. *Biophys. J.* **92,** 877–885
11. Zheng, L., Kostrewa, D., Bernèche, S., Winkler, F. K., and Li, X. D. (2004) The mechanism of ammonia transport based on the crystal structure of AmtB of *Escherichia coli*. *Proc. Natl. Acad. Sci. U.S.A.* **101,** 17090–17095
12. Boeckstaens, M., André, B., and Marini, A. M. (2008) Distinct transport mechanisms in yeast ammonium transport/sensor proteins of the Mep/Amt/Rh family and impact on filamentation. *J. Biol. Chem.* **283,** 21362–21370
13. Boussiba, S., Dilling, W., and Gibson, J. (1984) Methylammonium transport in *Anacystis nidulans* R-2. *J. Bacteriol.* **160,** 204–210
14. Hall, J. A., and Kustu, S. (2011) The pivotal twin histidines and aromatic

triad of the *Escherichia coli* ammonium channel AmtB can be replaced. *Proc. Natl. Acad. Sci. U.S.A.* **108,** 13270–13274
15. Kim, M., Zhang, Z., Okano, H., Yan, D., Groisman, A., and Hwa, T. (2012) Need-based activation of ammonium uptake in *Escherichia coli*. *Mol. Syst. Biol.* **8,** 616
16. Kleiner, D., and Fitzke, E. (1981) Some properties of a new electrogenic transport system: the ammonium (methylammonium) carrier from *Clostridium pasteurianum*. *Biochim. Biophys. Acta* **641,** 138–147
17. Ludewig, U., von Wirén, N., and Frommer, W. B. (2002) Uniport of NH_4^+ by the root hair plasma membrane ammonium transporter LeAMT1;1. *J. Biol. Chem.* **277,** 13548–13555
18. Søgaard, R., Alsterfjord, M., Macaulay, N., and Zeuthen, T. (2009) Ammonium ion transport by the AMT/Rh homolog TaAMT1;1 is stimulated by acidic pH. *Pflugers Arch.* **458,** 733–743
19. Ullmann, R. T., Andrade, S. L., and Ullmann, G. M. (2012) Thermodynamics of transport through the ammonium transporter Amt-1 investigated with free energy calculations. *J. Phys. Chem. B* **116,** 9690–9703
20. Walter, B., Küspert, M., Ansorge, D., Krämer, R., and Burkovski, A. (2008) Dissection of ammonium uptake systems in *Corynebacterium glutamicum*: mechanism of action and energetics of AmtA and AmtB. *J. Bacteriol.* **190,** 2611–2614
21. Andrade, S. L., Dickmanns, A., Ficner, R., and Einsle, O. (2005) Crystal structure of the archaeal ammonium transporter Amt-1 from *Archaeoglobus fulgidus*. *Proc. Natl. Acad. Sci. U.S.A.* **102,** 14994–14999
22. Blakey, D., Leech, A., Thomas, G. H., Coutts, G., Findlay, K., and Merrick, M. (2002) Purification of the *Escherichia coli* ammonium transporter AmtB reveals a trimeric stoichiometry. *Biochem. J.* **364,** 527–535
23. Gruswitz, F., Chaudhary, S., Ho, J. D., Schlessinger, A., Pezeshki, B., Ho, C. M., Sali, A., Westhoff, C. M., and Stroud, R. M. (2010) Function of human Rh based on structure of RhCG at 2.1 Å. *Proc. Natl. Acad. Sci. U.S.A.* **107,** 9638–9643
24. Li, X., Jayachandran, S., Nguyen, H. H., and Chan, M. K. (2007) Structure of the *Nitrosomonas europaea* Rh protein. *Proc. Natl. Acad. Sci. U.S.A.* **104,** 19279–19284
25. Lupo, D., Li, X. D., Durand, A., Tomizaki, T., Cherif-Zahar, B., Matassi, G., Merrick, M., and Winkler, F. K. (2007) The 1.3-Å resolution structure of *Nitrosomonas europaea* Rh50 and mechanistic implications for NH_3 transport by Rhesus family proteins. *Proc. Natl. Acad. Sci. U.S.A.* **104,** 19303–19308
26. Gruswitz, F., O'Connell, J., 3rd, and Stroud, R. M. (2007) Inhibitory complex of the transmembrane ammonia channel, AmtB, and the cytosolic regulatory protein, GlnK, at 1.96 Å. *Proc. Natl. Acad. Sci. U.S.A.* **104,** 42–47
27. Petrek, M., Otyepka, M., Banás, P., Kosinová, P., Koca, J., and Damborský, J. (2006) CAVER: a new tool to explore routes from protein clefts, pockets and cavities. *BMC Bioinformatics* **7,** 316
28. Javelle, A., Lupo, D., Zheng, L., Li, X. D., Winkler, F. K., and Merrick, M. (2006) An unusual twin-His arrangement in the pore of ammonia channels is essential for substrate conductance. *J. Biol. Chem.* **281,** 39492–39498
29. Javelle, A., Lupo, D., Ripoche, P., Fulford, T., Merrick, M., and Winkler, F. K. (2008) Substrate binding, deprotonation, and selectivity at the periplasmic entrance of the *Escherichia coli* ammonia channel AmtB. *Proc. Natl. Acad. Sci. U.S.A.* **105,** 5040–5045
30. Loqué, D., Mora, S. I., Andrade, S. L., Pantoja, O., and Frommer, W. B. (2009) Pore mutations in ammonium transporter AMT1 with increased electrogenic ammonium transport activity. *J. Biol. Chem.* **284,** 24988–24995
31. Soupene, E., van Heeswijk, W. C., Plumbridge, J., Stewart, V., Bertenthal, D., Lee, H., Prasad, G., Paliy, O., Charernnoppakul, P., and Kustu, S. (2003) Physiological studies of *Escherichia coli* strain MG1655: growth defects and apparent cross-regulation of gene expression. *J. Bacteriol.* **185,** 5611–5626
32. Inwood, W. B., Hall, J. A., Kim, K. S., Demirkhanyan, L., Wemmer, D., Zgurskaya, H., and Kustu, S. (2009) Epistatic effects of the protease/chaperone HflB on some damaged forms of the *Escherichia coli* ammonium channel AmtB. *Genetics* **183,** 1327–1340
33. Baba, T., Ara, T., Hasegawa, M., Takai, Y., Okumura, Y., Baba, M., Datsenko, K. A., Tomita, M., Wanner, B. L., and Mori, H. (2006) Construction of *Escherichia coli* K-12 in-frame, single-gene knockout mutants: the Keio collection. *Mol. Syst. Biol.* **2,** 2006.0008
34. Gutnick, D., Calvo, J. M., Klopotowski, T., and Ames, B. N. (1969) Compounds which serve as the sole source of carbon or nitrogen for *Salmonella typhimurium* LT-2. *J. Bacteriol.* **100,** 215–219
35. Neidhardt, F. C., Bloch, P. L., and Smith, D. F. (1974) Culture medium for enterobacteria. *J. Bacteriol.* **119,** 736–747
36. Bender, R. A., and Magasanik, B. (1977) Regulatory mutations in the *Klebsiella aerogenes* structural gene for glutamine synthetase. *J. Bacteriol.* **132,** 100–105
37. Soupene, E., He, L., Yan, D., and Kustu, S. (1998) Ammonia acquisition in enteric bacteria: physiological role of the ammonium/methylammonium transport B (AmtB) protein. *Proc. Natl. Acad. Sci. U.S.A.* **95,** 7030–7034
38. Zimmer, D. P., Soupene, E., Lee, H. L., Wendisch, V. F., Khodursky, A. B., Peter, B. J., Bender, R. A., and Kustu, S. (2000) Nitrogen regulatory protein C-controlled genes of *Escherichia coli*: scavenging as a defense against nitrogen limitation. *Proc. Natl. Acad. Sci. U.S.A.* **97,** 14674–14679
39. Epstein, W. (2003) The roles and regulation of potassium in bacteria. *Prog. Nucleic Acid Res. Mol. Biol.* **75,** 293–320
40. Rhoads, D. B., Waters, F. B., and Epstein, W. (1976) Cation transport in *Escherichia coli.* VIII. Potassium transport mutants. *J. Gen. Physiol.* **67,** 325–341
41. Dixon, M. (1953) The determination of enzyme inhibitor constants. *Biochem. J.* **55,** 170–171
42. Volkmer, B., and Heinemann, M. (2011) Condition-dependent cell volume and concentration of *Escherichia coli* to facilitate data conversion for systems biology modeling. *PLoS ONE* **6,** e23126
43. Javelle, A., Severi, E., Thornton, J., and Merrick, M. (2004) Ammonium sensing in *Escherichia coli*. *J. Biol. Chem.* **279,** 8530–8538
44. Boogerd, F. C., Ma, H., Bruggeman, F. J., van Heeswijk, W. C., García-Contreras, R., Molenaar, D., Krab, K., and Westerhoff, H. V. (2011) AmtB-mediated NH_3 transport in prokaryotes must be active and as a consequence regulation of transport by GlnK is mandatory to limit futile cycling of NH_4^+/NH_3. *FEBS Lett.* **585,** 23–28
45. Guether, M., Neuhäuser, B., Balestrini, R., Dynowski, M., Ludewig, U., and Bonfante, P. (2009) A mycorrhizal-specific ammonium transporter from *Lotus japonicas* acquires nitrogen release by arbuscular mycorrhizal fungi. *Plant Physiol.* **150,** 73–83
46. Neuhäuser, B., Dynowski, M., and Ludewig, U. (2009) Channel-like NH_3 flux by ammonium transporter AtAMT2. *FEBS Lett.* **583,** 2833–2838
47. Wang, S., Orabi, E. A., Baday, S., Bernèche, S., and Lamoureux, G. (2012) Ammonium transporters achieve charge transfer by fragmenting their substrate. *J. Am. Chem. Soc.* **134,** 10419–10427
48. Marini, A. M., Soussi-Boudekou, S., Vissers, S., and Andre, B. (1997) A family of ammonium transporters in *Saccharomyces cerevisiae*. *Mol. Cell. Biol.* **17,** 4282–4293
49. Booth, I. R. (1985) Regulation of cytoplasmic pH in bacteria. *Microbiol. Rev.* **49,** 359–378
50. Booth, I. R. (1999) The regulation of intracellular pH in bacteria. *Novartis Found. Symp.* **221,** 19–28; discussions 28–37
51. Capone, D. G. (2000) in *Microbial Ecology of the Oceans* (Kirchman, D.L., ed) pp. 455–493, John Wiley & Sons, New York
52. Millero, F. J. (2006) *Chemical Oceanography*, pp. 55–62, 3rd Ed., CRC Press, Boca Raton, FL
53. Walker, C. B., de la Torre, J. R., Klotz, M. G., Urakawa, H., Pinel, N., Arp, D. J., Brochier-Armanet, C., Chain, P. S., Chan, P. P., Gollabgir, A., Hemp, J., Hügler, M., Karr, E. A., Könneke, M., Shin, M., Lawton, T. J., Lowe, T., Martens-Habbena, W., Sayavedra-Soto, L. A., Lang, D., Sievert, S. M., Rosenzweig, A. C., Manning, G., and Stahl, D. A. (2010) *Nitrosopumilus maritimus* genome reveals unique mechanisms for nitrification and autotrophy in globally distributed marine crenarchaea. *Proc. Natl. Acad. Sci. U.S.A.* **107,** 8818–8823